ChemComm

Accepted Manuscript

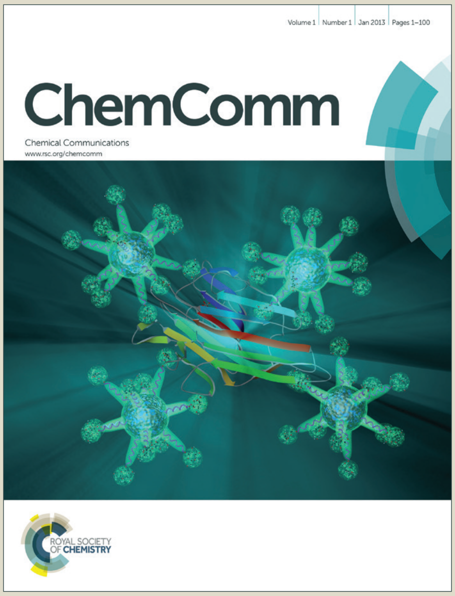

ROYAL SOCIETY OF CHEMISTRY

www.rsc.org/chemcomm

Cite this: DOI: 10.1039/c0xx00000x

www.rsc.org/xxxxxx

Communication

Bicomponent blend-directed amplification of alkyl chain effect on the 2D structures†

Yoshihiro Kikkawa,*[a] Manami Ishitsuka,[b] Ayumi Kashiwada[b] Seiji Tsuzuki,[a] and Kazuhisa Hiratani[a]

Received (in XXX, XXX) Xth XXXXXXXXX 20XX, Accepted Xth XXXXXXXXX 20XX

DOI: 10.1039/b000000x

Only one methylene unit difference in the long alkyl group of isobutenyl ether compounds is amplified by blending, resulting in the diversification of 2D structures, although each component formed individual 2D patterns, regardless of alkyl chain lengths. The 2D structures were revealed by using scanning tunneling microscopy at solid/liquid interface.

Fabrication of nano-sized patterns and objects has been attempted by applying both bottom-up and top-down approaches.[1] Particular to the single-nanoscale patterns, self-assembly, which is a spontaneous organization of molecules, plays definitive role as bottom-up strategy,[2] and can be used for the creation of various 2D patterns potentially applicable to nanoelectronics, molecular devices and lithographic techniques.[3] Integration of molecular building blocks in the physisorbed and chemisorbed monolayers has been characterized by using scanning tunneling microscopy (STM).[4]

To tune the 2D structures on a surface, directional intermolecular interaction sites such as hydrogen bonds and metal coordination have been conventionally introduced into the molecular building blocks. [5] In addition, relatively-weak van der Waals interaction of alkyl tails also allowed to provide various types of 2D patterns.[6] Among the alkyl chain effects, alternative change in the physical and chemical properties is well-known as odd-even effect, which has been discussed in terms of the steric repulsion of terminal methyl groups.[6b] Although there are a lot of reports on the odd-even effect,[7] to our knowledge, there is no previously-reported example that shows 2D structural modulation after blending of inert component against the alkyl chain length effect.

Controlled molecular organization and the following transformation of the nano-patterns on a surface will enable to achieve post-tunable properties and functions via the external stimuli, such as thermal treatment, metallation, blending the other component, and so on. Indeed, most of biological organizations are fundamentally based on the hybrid-assembled proteins exploiting the stimuli-responsive conformational and skeletal changes to accomplish the functional metamorphosis.[8] Mimicking such intelligent and elegant biological system, much attention has been paid for the fabrication of multi-component 2D structures because of inherent possibility of diversified nano-patterns as well as post-tunable properties and functions.[9]

In this contribution, we prepare the four kinds of isobutenyl ether compounds with alkyl tails connected by ester (**OC**$_n$) and carbamoyl (**CC**$_\mathbf{n}$) linkages with n = 15 and 16 (Fig. 1). The 2D structures are visualized by using STM at a highly oriented pyrolytic graphite (HOPG)/1-phenyloctane interface. In addition, effect of bicomponent blend on the 2D structures is examined ex situ and in situ.

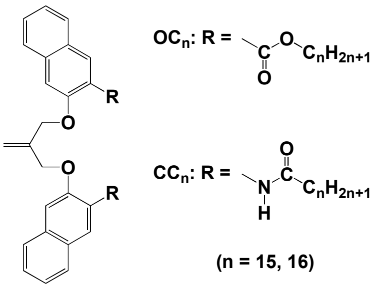

Fig. 1 Chemical structures of isobutenyl ether compounds, in which the alkyl chains are connected with ester (**OC**$_n$) and carbamoyl (**CC**$_\mathbf{n}$) groups (n = 15 and 16).

STM observations were performed for **OC**$_n$ and **CC**$_\mathbf{n}$ at HOPG/1-phenyloctane interface. Fig. 2 shows the STM images of **OC**$_{15}$ and **CC**$_{15}$. In each STM image, naphthalene and alkyl chain units were recognized as bright dots and dark lines, respectively. The **OC**$_{15}$ showed dumbbell shaped structures,[10] whereas linear structures were formed for **CC**$_{15}$, and this was the case for n=16 (Fig. S2 in ESI). Although interdigitated alkyl chains were found in both 2D structures of **OC**$_n$ and **CC**$_\mathbf{n}$, the different 2D structural features can be derived from the existence and non-existence of five-membered intramolecular hydrogen bonds in **CC**$_\mathbf{n}$ and **OC**$_n$, respectively (ESI).[11] This result indicates that the linkage of alkyl chain unit to the isobutenyl ether core part affected the 2D structure formation, although the number of carbon atoms in the alkyl chain units has less influence on it within the range of carbon numbers of 15 and 16.

---

[a] *National Institute of Advanced Industrial Science and Technology (AIST), Tsukuba Central 4, 1-1-1 Higashi, Tsukuba, Ibaraki 305-8562, Japan. Fax: +81-29-861-3029; Tel: +81-29-861-2955; E-mail: y.kikkawa@aist.go.jp*
[b] *Department of Applied Molecular Chemistry, College of Industrial Technology, Nihon University, 1-2-1 Izumi-cho, Narashino, Chiba 275-8575, Japan*

† Electronic Supplementary Information (ESI) available: Experimental detail, Additional STM images, Molecular models, and FT-IR spectra. See DOI: 10.1039/b000000x/

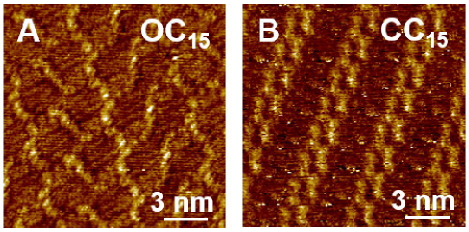

Fig. 2 STM images of **OC$_{15}$** (A) and **CC$_{15}$** (B) physisorbed at HOPG/1-phenyloctane interface. Molecular models and 2D structural features are shown in Fig. S2. Tunneling conditions: (A) **OC$_{15}$**, I = 2.2 pA, V = -620 mV; (B) **CC$_{15}$**, I = 1.5 pA, V = -530 mV.

Since the 2D structural differences due to the alkyl chain length were not found in each component, effect of blending on the 2D pattern formation was determined. First, ex situ blending, namely pre-blending before STM experiments was performed. Figs. 3, S3 and S4 in ESI show the STM images of **OC$_n$** and **CC$_n$** blends with various blend ratio. There was no concentration dependence on the 2D structure within the present experimental condition of 0.01–0.4 mM (see ESI). To our surprise, four types of the 2D structures were observed dependent on the blend ratio. In the case of **OC$_{15}$** ≥ **CC$_{15}$**, C3 symmetric star-like 2D patterns composed of six dumbbell-shaped frameworks were found throughout the HOPG surface (Fig. 3(A)). However, in the blends of **OC$_{15}$** < **CC$_{15}$**, lozenge-shaped patterns were formed (Fig. 3(B)). By contrast, twist-like morphology was found in the monolayer with **OC$_{16}$** > **CC$_{16}$** (Fig. 3(C)), whereas **OC$_{16}$** ≤ **CC$_{16}$** blend displayed only linear structure (Fig. 3(D)), which was identical to the 2D structure of only **CC$_n$**. There are two-types of twist-like structures with different periodicities, and they were arranged alternately (Fig. S4(G) and (H)). At the specific blend ratio, biphasic separation was transitionally found as shown in Fig. S4(D) and (I). Thus, these 2D structures were completely dependent on both alkyl chain length and blend ratio.[12] To the best of our knowledge, this is the first example that blending amplifies the alkyl chain length effect, resulting in the formation of various unprecedented 2D structures, which can be controlled by the blend ratio. In addition, it is noteworthy that the 2D patterns are tunable by only one CH_2 group difference in the alkyl chains. Unfortunately, the locations of each component in the blended 2D structure could not be identified because the difference between the two components of **OC$_n$** and **CC$_n$** is only the linkage of alkyl chain units to the basic skeleton of isobutenyl ether unit, and STM cannot detect and distinguish between two species. Therefore, plausible molecular models are tentatively depicted by using only **CC$_n$** molecular framework (Fig. S2). In all blend assemblies, alkyl chains of the components were interdigitated.

The great advantage of solid/liquid interface system is that post-blending is available on a HOPG surface, and therefore dynamic 2D structural changes can be followed by STM in situ. First, dumbbell-shaped 2D pattern formation in **OC$_{15}$** was confirmed as shown in Fig. S7(A), and a small amount of **CC$_{15}$** in 1-phenyloctane was added to already-existing drop of the **OC$_{15}$** on the HOPG, resulting in the formation of star-like structures (Fig. 4(A)). The interaction was too fast to capture the 2D structural change from dumbbell-shaped to star-like structures. On adding the excess amount of **CC$_{15}$** to the **OC$_{15}$** > **CC$_{15}$** blend, gradual structural change from star-like to lozenge-shaped morphology was visualized as shown in Fig. 4(B)–(D). Finally, almost whole area for STM imaging was occupied by the lozenge-shaped structure. The 2D pattern changed from the periphery of star-like structure, implying that the molecular components of **OC$_{15}$** > **CC$_{15}$** blend is gradually detached from the HOPG surface due to the equilibrium shift, and that the new

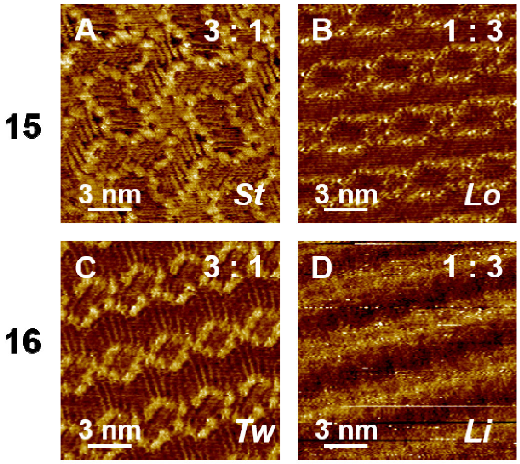

Fig. 3 STM images of **OC$_n$** and **CC$_n$** blends with different ratio (Total solute concentration is 0.2 mM). The blend ratio is shown in the right corner of each STM image in the order of **OC$_n$** : **CC$_n$**. The 2D structural feature is indicated as star-like (*St*; A), lozenge-shaped (*Lo*; B), twist-like (*Tw*; C), and linear structure (*Li*; D). Tunneling conditions: (A) I = 1.5 pA, V = -200 mV; (B) I = 2.0 pA, V = -300 mV; (C) I = 1.4 pA, V = -660 mV; (D) I = 2.0 pA, V = -660 mV.

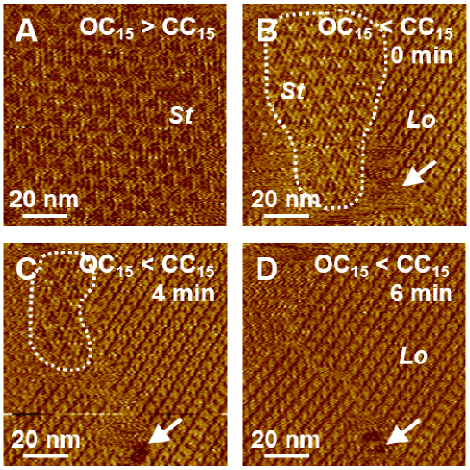

Fig. 4 In situ blending of **OC$_{15}$** with **CC$_{15}$**. In (A), the **CC$_{15}$** solution was added into the already-existing drop of **OC$_{15}$** on the HOPG surface to be the blend ratio of **OC$_{15}$** > **CC$_{15}$**. Then, further addition of **CC$_{15}$** solution to be **OC$_{15}$** < **CC$_{15}$** allowed to follow the time-dependent 2D structural change by the STM (C–F). The arrow in (B–D) indicates the same position during the STM imaging. Tunneling conditions: (A) I = 1.5 pA, V = -150 mV; (B–D) I = 2.0 pA, V = -280 mV.

molecular complex of **OC$_{15}$** < **CC$_{15}$** grows via surface-assisted assembly on a HOPG support to form lozenge-shaped structure. Further addition of **OC$_{15}$** allowed the formation of star-like structure, again. Such STM observation of time-dependent structural change was also available for **OC$_{16}$** and **CC$_{16}$** blends (see Fig. S8 in ESI). These results indicate that either **OC$_n$** or **CC$_n$** can be the trigger to switch the 2D structure from original shapes to different ones, and that post-tuning of 2D structure is possible by adding the other components.

To check whether the intermolecular hydrogen bond between -C=O in **OC$_n$** and -N-H in **CC$_n$** exist or not, the blend solution in chloroform was drop-cast on KBr plate, and FT-IR measurement was performed. Unexpectedly, no peak shift of -N-H stretch (3322 cm^{-1}) was observed in comparison to each blend component of **OC$_n$** and **CC$_n$** (see Fig. S9 in ESI), suggesting that intermolecular hydrogen bond is minor interaction in the present 2D blend assembly, although the FT-IR experiment was carried out in bulk.[13] On the basis of STM and FT-IR results, a plausible mechanism can be proposed as follows: van der Waals interaction between the alkyl chain units in **OC$_n$** and **CC$_n$** dominates the formation of interdigitated sub-structure with the support of HOPG. The arrangement of sub-structures is dependent on the blend ratio to form densely-packed 2D nanoarchitectures.

In nature, it is well-known that only a molecular-level slight change provides big differences in functions, morphologies, and so on. One of the examples is that the handedness of snails (clockwise and counter clockwise) is decided by only one genetic difference.[14] The other example is that productivity of microbial biodegradable polyester of polyhydroxyalkanoates (PHA) is improved in 50 times by a single mutation of PHA synthease gene from Ser to Thr at 325 position, and additional mutation from Glu to Lys at 481 position gives rise to 400-fold PHA synthesis compared to the wild-type.[15] In our present study, merely one CH$_2$ unit difference in the alkyl chains provided the drastic change in the 2D structures, which can be controlled by the blend ratio. Therefore, even one CH$_2$ group can maintain the 2D structural information, which is amplified and translated to the individual 2D patterns by blending.

In conclusion, unprecedented 2D structures were individually created at 1-phenyloctane/HOPG interface by the combinations of relatively weak van der Waals interaction and bicomponent blend of **OC$_n$** and **CC$_n$** (n = 15 and 16). Each component of **OC$_n$** and **CC$_n$** respectively displayed dumbbell-shaped and linear structures, irrespective of carbon numbers in the alkyl chain unit. However, on blending the **OC$_n$** and **CC$_n$**, completely different 2D structures compared to the original components were formed such as C3 symmetric star-like (**OC$_{15}$** ≥ **CC$_{15}$**), lozenge-shaped (**OC$_{15}$** < **CC$_{15}$**), twist-like (**OC$_{16}$** > **CC$_{16}$**), and linear structures (**OC$_{16}$** ≤ **CC$_{16}$**). These structural formations were dependent on both alkyl chain length (difference of only CH$_2$ unit!) and blend ratio. The present results would contribute to develop the post-tunable dynamic nano-patterns with unique orientations, and are significant to understand how the chemical structure of molecular building blocks including even one CH$_2$ unit difference affects the final 2D nano-architectures assembled on a surface.

Notes and references

1 A. Biswas, I. S. Bayer, A. S. Biris, T. Wang, E. Dervishi, F. Faupel, *Adv. Colloid Interface Sci.* 2012, **170**, 2.

2 (a) J. –M. Lehn, *Science* 2002, **295**, 2400. (b) G. M. Whitesides, B. Grzybowski, *Science* 2002, **295**, 2418-2421. (c) J. V. Barth, G. Costantini, K. Kern, *Nature* 2005, **437**, 671. (d) E. Gomar-Nadal, J. Puigmartí-Luis, D. B. Amabilino, *Chem. Soc. Rev.*, 2008, **37**, 490.

3 (a) J. Fritz, M. K. Baller, H. P. Lang, H. Rothuizen, P. Vettiger, E. Meyer, H. J. Guntherodt, C. Gerber, J. K. Gimzewski, *Science* 2000, **288**, 316. (b) Z. J. Donhauser, B. A. Mantooth, K. F. Kelly, L. A. Bumm, J. D. Monnell, J. J. Stapleton, D. W. Price, A. M. Rawlett, D. L. Allara, J. M. Tour, P. S. Weiss, *Science* 2001, **292**, 2303. (c) C. Tang, E. M. Lennon, G. H. Fredrickson, E. J. Kramer, C. J. Hawker, *Science* 2008, **322**, 429.

4 (a) R. K. Smith, P. A. Lewis, P. S. Weiss, *Prog. Surf. Sci*. 2004, **75**, 1. (b) K. E. Plass, A. L. Grzesiak, A. J. Matzger, *Acc. Chem. Res.* 2007, **40**, 287. (c) S. De Feyter, F. C. De Schryver, *J. Phys. Chem. B.* 2005, **109**, 4290.

5 (a) J. A. A. W. Elemans, S. Lei, S. De Feyter, *Angew. Chem. Int. Ed.* 2009, **48**, 7298. (b) C. –A. Palma, A. Ciesielski, M. Bonini, P. Samorì, in *Functional Supramolecular Architectures* (Eds. P. Samorì, F. Cacialli), Wiley-VCH, Weinheim, Germany 2011, Ch. 13.

6 (a) K. Tahara, S. Furukawa, H. Uji-i, T. Uchino, T. Ichikawa, J. Zhang, W. Mandouh, M. Sonoda, F. C. De Schryver, S. De. Feyter, Y. Tobe, *J. Am. Chem. Soc.* 2006, **128**, 16613. (b) F. Tao, S. L. Bernasek, *Chem. Rev.* 2007, **107**, 1408. (c) Y. Kikkawa, *Polym. J.* 2013, **45**, 255.

7 (a) X. Weng, C. Y. Li, S. Jin, D. Zhang, J. Z. Zhang, F. Bai, F. W. Harris S. Z. D. Cheng, *Macromolecules* 2002, **35**, 9678. (b) R. Colorado, Jr., T. R. Lee, *Langmuir* 2003, **19**, 3288. (c) P. T. Mikulski, L. A. Herman, J. A. Harrison, *Langmuir* 2005, **21**, 12197. (d) D. A. M. Egbe, C. Ulbricht, T. Orgis, B. Carbonnier, T. Kietzke, M. Peip, M. Metzner, M. Gericke, E. Birckner, T. Pakula, D. Neher U. –W. Grummt, *Chem. Mater.* 2005, **17**, 6022. (e) Y. Sonoda, M. Goto, S. Tsuzuki N. Tamaoki, *J. Phys. Chem. A*, 2006, **110**, 13379. (f) K. Omori, Y. Kikkawa, M. Kanesato, K. Hiratani, *Chem. Commun.* 2010, **46**, 8008. (g) L. Xu, X. Miao, B. Zha, K. Miao W. Deng, *J. Phys. Chem. C*. 2013, **117**, 12707. (h) Y. Xue, M. K. Kim, T. Pašková, M. B. Zimmt, *J. Phys. Chem. B* 2013, **117**, 15856. (i) E. Ghijsens, O. Ivasenko, K. Tahara, H. Yamaga, S. Itano, T. Balandina, Y. Tobe, S. De Feyter, *ACS Nano* 2013, **7**, 8031. (j) R. Plamont, Y. Kikkawa, M. Takahashi, M. Kanesato, M. Giorgi, A. C. K. Shun, C. Roussel, T. S. Balaban, *Chem. Eur. J.* 2013, **19**, 11293. (k) E. Badea, B. Nowicka G. Della Gatta, *J. Chem. Thermodyn.* 2014, **68**, 90.

8 For example: A. Miyazawa, Y. Fujiyoshi, N. Unwin, *Nature* 2003, **423**, 949.

9 (a) S. De Feyter, A. Miura, S. Yao, Z. Chen, F. Würthner, P. Jonkheijm, A. P. H. J. Schenning, E. W. Meijer, F. C. De Schryver, *Nano Lett.* 2005, **5**, 77. (b) S. Lei, M. Surin, K. Tahara, J. Adisoejoso, R. Lazzaroni, Y. Tobe, S. De Feyter, *Nano Lett.* 2008, **8**, 2541. (c) L. Wang, Q. Chen, G. B. Pan, L. J. Wan, S. Zhang, X. Zhan, B. H. Northrop, P. J. Stang, *J. Am. Chem. Soc.* 2008, **130**, 13433. (e) K. S. Mali, J. Adisoejoso, E. Ghijsens, I. De Cat, S. De Feyter, *Acc. Chem. Res.* 2012, **45**, 1309.

10 Plausible molecular models are shown in Fig. S2 in ESI. In the case of **OC$_n$**, some vacant space in the lattice can be filled with 1-phenyloctane. Such coadsorption of solvent molecules are reported in following literatures: (a) W. Mamdouh, H. Uji-I, J. S. Ladislaw, A. E. Dulcey, V. Percec, F. C. De Schryver, S. De Feyter, *J. Am. Chem.*

Soc. 2006, **128**, 317. **(**b) Y. Kikkawa, K. Omori, M. Takahashi, M. Kanesato, K. Hiratani, *Org. Biomol. Chem.* 2012, **10**, 8087.

11 Relatively strong six-membered hydrogen bonds formed in the isobutenyl compounds possessing amide-linked alkyl tails didn't allow the accommodation of interdigitated alkyl chains in the 2D structures. (a) K. Omori, Y. Kikkawa, M. Kanesato, K. Hiratani, *Chem. Lett.* 2010, **39**, 1039. (b) K. Omori, Y. Kikkawa, H. Tokuhisa, M. Kanesato, K. Hiratani, *Colloids Surf. A*, 2010, **356**, 58.

12 The heterogeneous blend with different alkyl chain length didn't exhibit such structural diversification (see ESI).

13 Further discussion on the intermolecular hydrogen bond is given in ESI from the viewpoint of stabilization energy.

14 R. Ueshima, T. Asami, *Nature*, 2003, ***425***, 679.

15 K. Takase, S. Taguchi, Y. Doi, *J. Biochem.* 2003, **133**, 139.

A graphical abstract

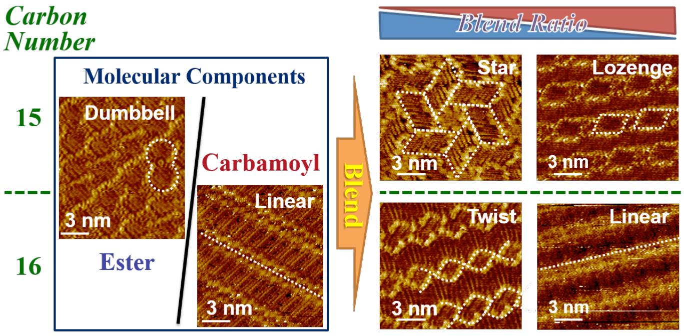

The 2D structures of bicomponent blends in isobutenyl compounds were observed by using scanning tunneling microscopy at solid/liquid interface. Amplification of alkyl chain effect was found on the 2D structures.